

Effect of interfacial states on the binding energies of electrons and holes in InAs/GaAs quantum dots

A. J. Williamson and Alex Zunger

National Renewable Energy Laboratory, Golden, Colorado 80401

(Received 24 April 1998)

The interface between an InAs quantum dot and its GaAs cap in “self-assembled” nanostructures is non-homogeneously strained. We show that this strain can lead to localization of a GaAs-derived X_{1c} -type interfacial electron state. As hydrostatic pressure is applied, this state in the GaAs barrier turns into the conduction-band minimum of the InAs/GaAs dot system. Strain splits the degeneracy of this X_{1c} state and is predicted to cause electrons to localize in the GaAs barrier above the pyramidal tip. Calculation (present work) or measurement (Itskevich *et al.*) of the emission energy from this state to the hole state can provide the hole binding energy, $\Delta_{\text{dot}}^{(h)}$. Combining this with the zero-pressure electron-hole recombination energy gives the electron binding energy, $\Delta_{\text{dot}}^{(e)}$. Our calculations show $\Delta_{\text{dot}}^{(h)} \sim 270$ meV (weakly pressure dependent) and $\Delta_{\text{dot}}^{(e)} \sim 100$ meV at $P=0$. The measured values are $\Delta_{\text{dot}}^{(h)} \sim 235$ meV (weakly pressure dependent) and $\Delta_{\text{dot}}^{(e)} \sim 50$ meV at $P=0$. We examine the discrepancy between these values in the light of wave-function localization and the pressure dependence of the hole binding energy. [S0163-1829(98)06635-1]

The interest in potential *optical* applications of semiconductor quantum dots has concentrated attention almost entirely on their direct gap electronic states, i.e., those derived from the Γ point of the bulk band structure, the Γ_{1c} -derived electron states and Γ_{15v} -derived hole states. There are however, several interesting quantum dot situations in which the lowest energy electron states of dots are derived from the X_{1c} point. These include (i) Si quantum dots,¹ and SiGe nanostructures embedded in Si,² (ii) InP nanostructures embedded within GaP (Refs. 3 and 4), and (iii) InAs nanostructures embedded in GaAs at a hydrostatic pressure above the $\Gamma_{1c}-X_{1c}$ transition.⁶ In some of these cases, [e.g., (ii) and (iii)], the resulting band alignment can be type II (indirect) in both reciprocal and real space, with holes confined to Γ -like states of the dot and electrons in X -derived states of the barrier. When a lattice mismatch between the dot and the barrier materials also exists, the resulting strain field can lead to localization of these X -derived electron states.^{2,4} This can be seen qualitatively by considering the simple case of an isotropic *spherical* inclusion in an isotropic matrix as originally derived in 1956 by Eshelby⁵ to first order in the lattice mismatch, $\epsilon_m = (a_i - a_m)/a_m$, where a_i and a_m are the lattice constants of the inclusion and the matrix, respectively. Eshelby showed that inside the sphere, only uniform hydrostatic strain exists,

$$\epsilon_{in} = \epsilon_m \left(\frac{1}{\gamma} - 1 \right), \quad (1)$$

where $\gamma = 1 + 2B_m(1 - 2\nu_m)/[B_i(1 + \nu_m)]$, and where B_i and B_m represent the bulk moduli of the inclusion and the matrix and ν_m is the Poisson ratio of the matrix. In the surrounding matrix however, the strain has both a radial (rad) and tangential (tan) component, given by

$$\begin{aligned} \epsilon_{\text{rad}}(r) &= -2 \frac{\epsilon_m}{\gamma} \left(\frac{R}{r} \right)^3, \\ \epsilon_{\text{tan}}(r) &= \frac{\epsilon_m}{\gamma} \left(\frac{R}{r} \right)^3. \end{aligned} \quad (2)$$

This spherical geometry is unique in that the strain decays with distance r . This decay is absent in the equivalent planar (quantum well) geometry. If the conduction-band minimum of the constrained barrier material is X_{1c} , as is the case on Si and GaP at ambient pressure, or GaAs above 43 kbar, then this radial and tangential strain will split the triply degenerate X_{1c} . This splitting is most significant at the interface between the spherical inclusion and the matrix due to the r^{-3} decay of the strain away from the interface. At this interface, the splitting can be strong enough to drive the lowest lying X_{1c} -derived state in the matrix below the lowest lying electron state in the sphere, producing a type II alignment. The predictions of this simple model were recently confirmed via atomistic calculations of spherical InP dots embedded within a GaP matrix.⁴ In this system, the X_{1c} -derived state of the GaP barrier is driven below the Γ_{1c} state of the InP quantum dot, producing a predicted type II alignment in both real and reciprocal space.

In this paper, we study InAs quantum dots, embedded within a GaAs barrier, under hydrostatic pressure, which was recently experimentally studied.⁶ Above a critical pressure, P_c , bulk GaAs is known⁷ to become indirect with an X_{1c} -like conduction-band minimum (CBM). The nonhydrostatic strain at the InAs/GaAs interface is then expected to split this X_{1c} CBM of GaAs. The band alignment is then expected to be type II in real space, in a similar fashion to the InP/GaP (Ref. 4) and SiGe/Si (Ref. 2) systems described above. In a recent paper, Itskevich *et al.*⁶ have studied these InAs/GaAs systems under pressures up to 100 kbar and they have observed evidence for the expected type II band alignment. They have also suggested an innovative method for deducing the electron and hole binding energies, $\Delta_{\text{dot}}^{(e)}$ and $\Delta_{\text{dot}}^{(h)}$ from their high pressure optical measurements. These binding energies are central spectroscopic quantities in quantum nanostructures and a method for directly measuring them would prove extremely useful. However, as we will see below, the existence of interfacial wave-function localization⁴ due to the response of the GaAs X_{1c} state to the Eshelby strain introduces a complication that requires a theoretical treatment.

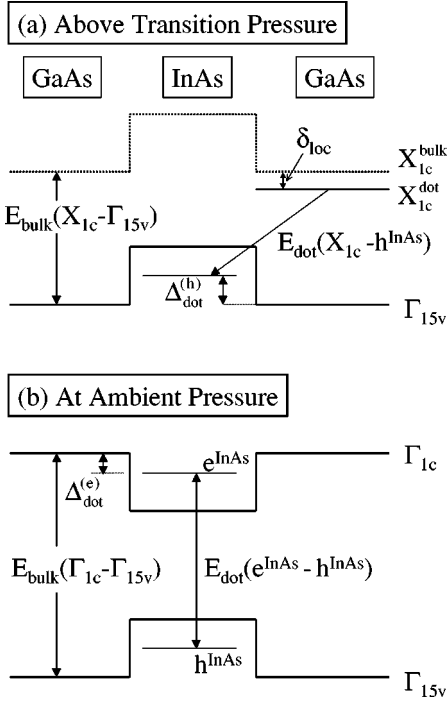


FIG. 1. Schematic band alignment of GaAs/InAs. See text and Eqs. (1)–(3) for explanation of symbols.

The method of Itskevich *et al.* assumes that above the critical pressure P_c , the emission takes place from the X_{1c}^{dot} level in the GaAs barrier, to the confined hole state, h^{InAs} , with an emission energy, $E_{dot}(X_{1c}^{GaAs} - h^{InAs}; P)$. Combining this value with the bulk GaAs indirect transition energy at this pressure, $E_{bulk}(X_{1c}^{GaAs} - \Gamma_{15v}^{GaAs}; P)$ the hole binding energy within the dot, $\Delta_{dot}^{(h)}(P)$, can be obtained from Fig. 1(a)

$$\Delta_{dot}^{(h)}(P) = E_{bulk}(X_{1c}^{GaAs} - \Gamma_{15v}^{GaAs}; P) - [E_{dot}(X_{1c}^{dot} - h^{InAs}; P) + \delta_{loc}(P)]. \quad (3)$$

This approach assumes that the emitting state X_{1c}^{dot} has precisely the energy of the threefold degenerate X_{1c} level in bulk GaAs under pressure P , i.e., that it is an extended Bloch state. This neglects the Eshelby strain that could exist at the GaAs-InAs interface, and the ensuing wave-function localization at the interface. This localization could shift the emitting state [Fig. 1(a)]. An extra correction term $\delta_{loc}(P)$, is therefore included in Eq. (3) to allow for emission from the ‘‘split X_{1c} state,’’ called X_{1c}^{dot} , rather than from bulk X_{1c}

$$\delta_{loc}(P) = E(X_{1c}^{GaAs} - X_{1c}^{dot}; P). \quad (4)$$

The electron binding energy $\Delta_{dot}^{(e)}(P)$, can then be determined [Fig. 1(b)] by subtracting from the zero-pressure direct gap of GaAs the measured zero-pressure electron-hole recombination energy $E_{dot}(e^{InAs} - h^{InAs}; P=0)$, and the zero-pressure hole confinement energy:

$$\Delta_{dot}^{(e)} = E_{bulk}(\Gamma_{1c}^{GaAs} - \Gamma_{15v}^{GaAs}; P=0) - E_{dot}(e^{InAs} - h^{InAs}; P=0) - \Delta_{dot}^{(h)}(P=0). \quad (5)$$

Since Eq. (3) gives the hole confinement energy at $P > P_c$, one has to obtain the zero-pressure value needed in Eq. (5) from

$$\Delta_{dot}^{(h)}(P=0) = \Delta_{dot}^{(h)}(P) + \frac{\partial \Delta_{dot}^{(h)}}{\partial P} \cdot \Delta P, \quad (6)$$

which requires knowledge of the deformation potential of the hole binding energy $\partial \Delta_{dot}^{(h)}/\partial P$.

Itskevich *et al.* took (i) $\delta_{loc}(P) = 0$ in Eq. (4) and (ii) they assumed a linear extrapolation of the pressure dependence for the photoluminescence emission from the X state to approximate $\partial \Delta_{dot}^{(h)}/\partial P = 1.0$ meV/kbar in Eq. (6). Using these two approximations, they obtain⁶

$$\begin{aligned} \Delta_{dot}^{(h)}(P=53 \text{ kbar}) &= 0.290 \text{ eV}, \\ \Delta_{dot}^{(h)}(P=0 \text{ kbar}) &= 0.235 \text{ eV}, \\ \Delta_{dot}^{(e)}(P=0 \text{ kbar}) &= 0.030 \text{ eV}, \end{aligned} \quad (7)$$

for their InAs/GaAs pyramidal dots, which they estimate⁸ to have a base of 150 \AA and a height of 15 \AA .

We have performed calculations of the electron and hole binding energy in a pyramidal InAs dot, embedded within a GaAs barrier as a function of pressure. These calculations include a full atomistic description of both the extended hydrostatic pressure and the nonhomogeneous strain profile of the system, allowing us to establish the extent of the Eshelby strain-induced wave-function localization. Our method is based on direct diagonalization of an empirical pseudopotential Hamiltonian.^{9–11} We calculate the electronic structure of an InAs pyramidal dot with the same base:height ratio (base = 100 \AA , height = 10 \AA) as Ref. 6, to obtain all the quantities appearing in Eqs. (3)–(6). We use an analytic form of pseudopotential, designed to build in the effects of strain, that is fitted¹⁰ to experimental band gaps, deformation potentials and effective masses. The atomic positions were calculated by relaxing all the atoms in the InAs pyramid and GaAs barrier to their minimum strain energy values, using the valence force field elastic energy functional.¹² The near-edge eigenstates of this pseudopotential Hamiltonian, expanded within a plane-wave basis, were calculated using the ‘‘folded spectrum method.’’¹¹ The calculations were performed for values of the GaAs lattice constant of 5.653, 5.555, 5.528, and 5.502 \AA . We then calculate the volume derivatives $\partial \epsilon/\partial V$ of the dot-energy levels and report results for the pressure derivatives $\partial \epsilon/\partial P$, obtained from $B^{-1}(V \partial \epsilon/\partial V)$, where V is the volume and B is the bulk modulus. Although the bulk modulus of dots can differ from the bulk value, it has not been accurately determined for this system and we therefore use the bulk GaAs value of $B = 75$ GPa. Using this bulk modulus, the above lattice constants correspond to applied hydrostatic pressures of 0, 39, 50, and 60 kbar.

Table I summarizes the calculated quantities appearing in Eqs. (3)–(5). Figure 2 shows the electron wave functions at $P=0$ and $P=60$ kbar in both real and reciprocal space. These calculations reveal three specific findings.

(i) There are interface-localized electron states in strained InAs/GaAs dots. These can be seen in the plots in Fig. 2. At

TABLE I. Pseudopotential and experimental results for all quantities in Fig. 1 and Eqs. (3)–(5). Pressures are in kbar, energies in eV.

Quantity	Pseudopotential calculations				Expt. ⁶
	$P=0$	$P=39$	$P=50$	$P=60$	
Holes					
$X_{1c}^{\text{GaAs}} - \Gamma_{15v}^{\text{GaAs}}$	1.999	1.912	1.882	1.850	1.935($P=53$)
$X_{1c}^{\text{dot}} - h^{\text{InAs}}$			1.554	1.528	1.645($P=53$)
δ_{loc}			0.037	0.021	
$\Delta_{\text{dot}}^{(h)}(P)$	0.271	0.274	0.291	0.301	0.290($P=53$)
Electrons					
$\Gamma_{1c}^{\text{GaAs}} - \Gamma_{15v}^{\text{GaAs}}$	1.548	1.954	2.064	2.172	1.519 ($P=0$)
$e^{\text{InAs}} - h^{\text{InAs}}$	1.180	1.497	1.554	1.528	1.255 ($P=0$)
$\Delta_{\text{dot}}^{(h)}(P)$	0.271	0.274	0.291	0.301	0.235 ($P=0$)
$\Delta_{\text{dot}}^{(e,\Gamma)}$	0.097	0.183	~ 0.206		0.029

$P=0$ the ground electron state is confined *within* the InAs dot [Fig. 2(a)], while at the pressure where the GaAs barrier undergoes a $\Gamma_{1c} \rightarrow X_{1c}$ transition, the GaAs/InAs interfacial strain produces a strain-split, *localized* X_{1c} state [Fig. 2(b)] localized *outside* the dot, above its tip. The energy of this state differs in energy by 0.024 eV from a Bloch-extended bulk GaAs X_{1c} state obtained in our calculation at a position far away from the dot, where the Eshelby strain [Eqs. (1)–(2)] has decreased to zero. The *hole* states do not significantly change their character with pressure and are always localized within the dot. Our directly calculated values at 60 kbar (see Table I) for Eq. (3) are

$$\Delta_{\text{dot}}^{(h)}(P=60) = 1.850 - 1.528 - 0.021 = 0.301 \text{ eV} \quad (8)$$

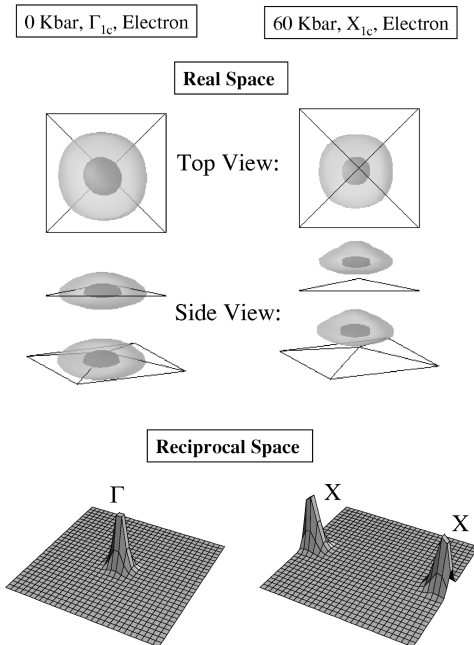


FIG. 2. Calculated wave functions squared of a pyramidal InAs dot (base=100 Å, height=10 Å). In real space isosurfaces are shown at 25% (light) and 75% (dark) of the maximum value. In reciprocal space the momentum space projection in the $k_y=0$ plane of the zinc-blende Brillouin zone are shown.

and for Eq. (5)

$$\Delta_{\text{dot}}^{(e)}(P=0) = 1.548 - 1.180 - 0.271 = 0.097 \text{ eV}. \quad (9)$$

For a larger dot (base=150 Å, height=15 Å) we obtain $\Delta_{\text{dot}}^{(h)}(P=60) = 0.338$ and $\Delta_{\text{dot}}^{(e)}(P=0) = 0.137$ eV. Thus, the approximation $\delta_{\text{loc}}=0$ used in Ref. 6 results in an *overestimate* of the hole binding energy $\Delta_{\text{dot}}^{(h)}$, and hence an *underestimate* of the electron binding energy $\Delta_{\text{dot}}^{(e)}(P=0)$, of 0.021 eV.

(ii) *Above* the $\Gamma_{1c} \rightarrow X_{1c}$ transition the hole binding energy does indeed decrease nearly linearly with pressure as assumed in Ref. 6. However, *below* the transition pressure, the hole binding energy is almost independent of pressure. Thus, the approximation $\partial \Delta_{\text{dot}}^{(h)} / \partial P = 1.0$ meV kbar⁻¹ results in an *underestimate* of the hole binding energy at $P=0$ and hence an *overestimate* of the equilibrium electron binding energy of 0.032 eV.

(iii) Table I shows the calculated values for the pressure dependence of the band gaps of bulk GaAs, InAs, and the GaAs embedded InAs quantum dot are 11.1, 9.0, and 8.0 meV/kbar, in excellent agreement with the measured values of 10.7,⁷ 10.0,⁷ and 8.0.⁶ The calculated value for the red shift of the emission above the critical pressure of -2.6 meV/kbar also shows excellent agreement with the measured value of -2.4 ± 0.2 meV/kbar. This red shift is attributed to emission from electrons in the X_{1c} -derived state. We also calculate a pressure dependence of the hole binding energy of 1.3 meV/kbar above the critical pressure and 0.5 meV/kbar below the critical pressure. The measured value⁶ above the critical pressure is approximately 1.0 meV/kbar.

To understand the origin of the shift, δ_{loc} , between the X_{1c} state of bulk GaAs and the X_{1c} state of the dot [Fig. 1(a)] we show in Fig. 2 the projection of the calculated electron dot wave functions at $P=0$ and $P=60$ kbar into the zincblende Brillouin zone, using the method described in Ref. 13. This projection reveals that the lowest energy electron state at $P=0$ is Γ derived, while at $P=60$ kbar this state is X derived. The highest energy hole states at both $P=0$ and $P=60$ kbar are Γ derived.

The localization of the X_{1c} -like electron state at $P=60$ kbar is due to the interface-induced strain described

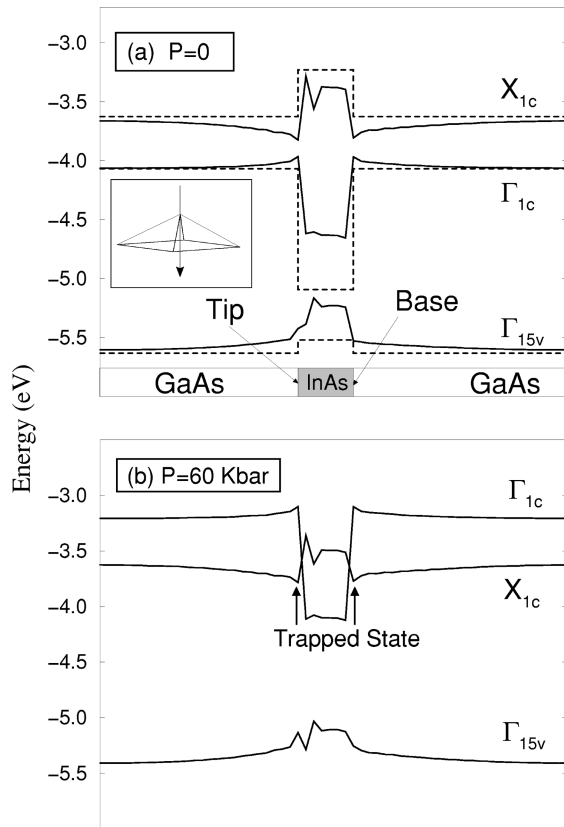


FIG. 3. Band offsets between GaAs and InAs at the Γ_{15v} , Γ_{1c} , and X_{1c} points at (a) zero pressure and (b) 60 kbar. Dashed (solid) lines indicate the unstrained (strained) offsets.

earlier. In Fig. 3, we use atomistic calculations to illustrate the effects on the band offsets of applying hydrostatic pressure to a GaAs embedded, strained InAs *pyramidal* quantum dot. The *unstrained* band offsets between GaAs and InAs are shown as dashed lines at zero pressure in Fig. 3(a). They show that at $P=0$ the natural GaAs/InAs offsets allow InAs to act as a “well” for both the conduction-band Γ_{1c} electrons and the valence-band Γ_{15v} holes (a “type I” offset). The solid lines in Fig. 3(a) show the offsets subject to the local strain $\epsilon(\mathbf{R})$, plotted along a [001] direction down through the tip of the InAs pyramid (see inset). We obtain the position-dependent strained offsets by discretizing the

GaAs/InAs nanostructure into “cells” with position vector \mathbf{R} and then performing 60 bulk band-structure calculations of InAs and GaAs, thus obtaining the bulk eigenvalues $E_{nk}[\epsilon(\mathbf{R})]$ for band n at wave vector k within each cell, using the strained In-As or Ga-As bond geometry in that cell.¹⁴ These solid lines in Fig. 3(a) show that far from the dot where the strain is small, the offsets approach the unstrained value, however the compressive strain within the InAs dot, increases the valence-band offset from 0.11 to 0.41 eV (allowing more confined hole states) and decreases the conduction-band offset from 1.01 to 0.55 eV (reducing the number of confined electron states).

Figure 3(b) shows the band offsets under 60 kbar of pressure. The GaAs barrier material has already undergone a conduction band $\Gamma_{1c} \rightarrow X_{1c}$ crossing, while the InAs remains direct. We observe that the strained band offset for X_{1c} electrons has developed *local minima* (indicated by arrows) just above the tip and below the base of the InAs dot. The development of these minima is principally due to the splitting of the triply degenerate X_{1c} -derived states by the epitaxial strain at the interface between the dot and the barrier as predicted by Yang *et al.*² It is within these minima that the lowest energy conduction state localizes. This leads to trapping of the electron wave function at the interface, and to a lowering of the energy level relative to the bulk GaAs X_{1c} level.

In conclusion, our pseudopotential calculations show that the InAs/GaAs interfacial strain leads to the development of a trough in the X_{1c} band offset, just above the tip and below the base of the InAs dot. At hydrostatic pressures where the GaAs barrier has an X_{1c} conduction-band minimum, an electron is trapped and localized in this trough. These results suggest that one needs to know this interface localization energy (e.g., from calculation) before the method proposed in Ref. 6 can yield accurate electron and hole binding energies.

We thank L. Eaves and A. Polimeni for sharing Ref. 6 prior to publication and for a useful discussion of these results. This work was supported by the DOE-Basic Energy Sciences, Division of Materials Science, under Contract No. DE-AC36-83CH10093. Calculations were performed using the Cray T3E at the National Energy Research Scientific Computing Center.

¹L. W. Wang and A. Zunger, in *Semiconductor Nanoclusters*, edited by P. V. Kamat and D. Meisel (Elsevier Science, Amsterdam, 1996).

²M. Yang, J. C. Sturm, and J. Prevost, *Phys. Rev. B* **56**, 1973 (1997).

³N. Carlsson, W. Seifert, A. Petersson, P. Castrillo, M. E. Pistol, and L. Samuelson, *Appl. Phys. Lett.* **25**, 3093 (1994).

⁴A. J. Williamson, A. Zunger, and A. Canning, *Phys. Rev. B* **57**, R4253 (1998).

⁵J. D. Eshelby, *J. Appl. Phys.* **25**, 255 (1954).

⁶I. Itskevich, S. Lyapin, I. Troyan, P. Klipstein, L. Eaves, P. Main, and M. Henini, *Phys. Rev. B* **58**, R4250 (1998).

⁷D. Wolford and J. Bradley, *Solid State Commun.* **53**, 1069 (1985); S. Ernst, A. Goni, K. Syassen, and M. Cardona, *Phys. Rev. B* **53**, 1287 (1996).

⁸A. Polimeni and L. Eaves (private communication).

⁹A. Zunger, *MRS Bull.* **23**, 35 (1998).

¹⁰A. J. Williamson, J. Kim, L. W. Wang, S.-H. Wei, and A. Zunger (unpublished).

¹¹L. W. Wang and A. Zunger, *J. Chem. Phys.* **100**, 2394 (1994).

¹²P. Keating, *Phys. Rev.* **145**, 637 (1966).

¹³L. W. Wang and A. Zunger, *Phys. Rev. B* **56**, 12 395 (1997).

¹⁴The results in Table I are independent of the construct in Fig. 3, which is purely for illustration purposes.